Granular Micro-Structure and Avalanche Precursors

L. Staron*, F. Radjai & J.-P. Vilotte

Department of Applied Mathematics and Theoretical Physics, Cambridge CB3 0WA, UK.

Laboratoire de Mécanique et Génie Civil, Montpellier 34095 Cx, France.

Institut de Physique du Globe de Paris, Paris 75252 Cx5, France.

Using numerical simulation, we show the existence of a sharp transition in the state of a granular slope few degrees before the angle of avalanche, involving the packing micro-structure and avalanche precursors. Interestingly, this transition coincides with the transition to metastability observed experimentally. This questions the emergence of new correlation lengths in relation with this sharp modification of the pile internal state.

1 INTRODUCTION

The stability of granular slopes is related to the existence of two angles. The static angle of avalanche θ_c characterizes the maximum slope angle compatible with static equilibrium. Equivalently, θ_c is the slope angle for which slope failure and surface avalanche are incipient. The dynamical angle of repose θ_d is the angle at which the surface of the flow is stabilized after a surface avalanche was triggered, with $\theta_d < \theta_c$. The angle of hysteresis, defined as the slope interval $[\theta_d, \theta_c]$ is typically of few degrees.

The value of θ_c reflects the effective properties of static friction of the packing. It is related to the microscopic friction acting at contacts and the geometrical effects due to the shape of the grains. The angle of avalanche is thus dependent on the organization of the packing at the grains scale, and is likely to be sensitive to its intrinsic disorder. This sensitivity is apparent when measuring the value of θ_c for one given granular medium over successive avalanches: θ_c is not mono-valued, but distributed in a slope interval of few degrees. In this slope interval the trigger of an avalanche is possible everywhere, suggesting a metastable state.

The metastability of granular slopes approaching the angle of avalanche has been investigated experimentally. Daerr $\&$ Douady (Daerr & Douady 1999) have measured the size of the perturbation necessary to trigger a surface flow depending on the slope θ of the surface. They found that the size of the perturbation tends to zero when the slope tends towards θ_c, and that no surface flow can be triggered for $\theta < \theta_d$, thus characterising the slope metastability as a sub-critical

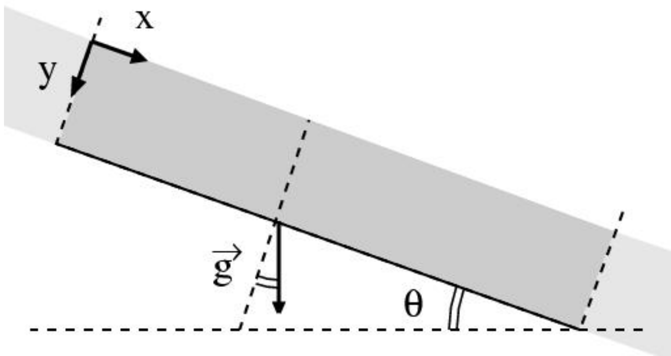

Figure 1. A periodic granular pile is driven towards stability limit by constant tilt under gravity.

transition. Other experiments show that a perturbation of given size applied to a granular pile affects an increasing area of the pile when the latter evolves towards θ_c (Deboeuf *et al* 2003).

These experiments show a profound modification of the state of the pile evolving towards stability limit, which effect is to increase the susceptibility of the pile to avalanching. However, beyond the observation of a metastable state in $[\theta_d, \theta_c]$, the precise analysis of the state of the granular pile in this interval escapes the experimental tools. In this contribution, we investigate the modification of the internal state of a granular slope using numerical simulation. We are thus able to show a sharp transition in the stress state of the pile for a slope θ few degrees lower than θ_c. This transition coincides with a critical mobilization of contact friction and the emergence of friction induced instabilities, and also coincides with the onset of dilatancy, which are all strong precursors of the destabilization.

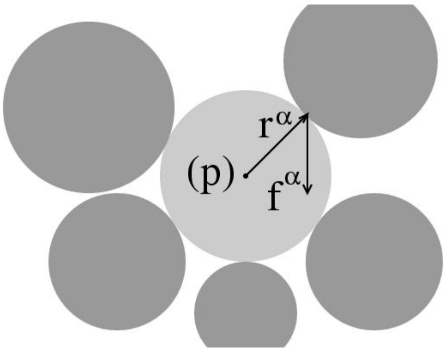

Figure 2. Grain p involved in contacts α with its neighbours; $\boldsymbol{r}^\alpha$ is the vector position of the contact α, and $\boldsymbol{f}^\alpha$ is the force transmitted at the contact α.

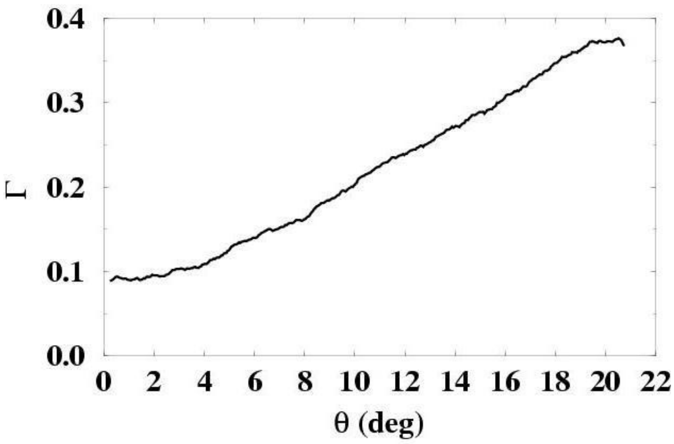

Figure 3. Evolution of the macroscopic stress ratio $\Gamma = Q/P$ as a function of the slope angle θ. The stability limit ocurres for $\theta = \theta_c \simeq 19.5$, for which the stress ratio reaches the limit value $\Gamma_c \simeq 0.36$.

2 NUMERICAL SIMULATION

We have applied the contact dynamics algorithm (Jean & Moreau 1992) in 2D to simulate a periodic granular pile composed of 10000 grains with diameter D distributed in a small interval so that $D_{max}/D_{min} = 1.5$, preventing long range crystal-like ordering of the packing. The pile is built by a random rain of grains in the gravity field; its width is $200D$ and his height is $\simeq 40D$. The grains are perfectly rigid and interact through a simple Coulomb friction involving the microscopic coefficient of friction μ at the contacts between the grains. The pile is tilted at a constant rotation rate in the gravity field so that the slope θ of its free surface increases slowly from initially 0 to the static angle of avalanche θ_c (Figure 1). The quasi-static evolution towards avalanching is the subject of what follows.

3 MULTI-SCALE ANALYSIS OF THE STRESS

3.1 *Definition*

To evaluate the level of stress applied to any volume of the packing, we use the concept of grains moment tensor defined in (Moreau 1997). We consider a grain p involved in N_α contacts with neighboring grains, and submitted to the forces $\boldsymbol{f}^\alpha$ applied at the contact

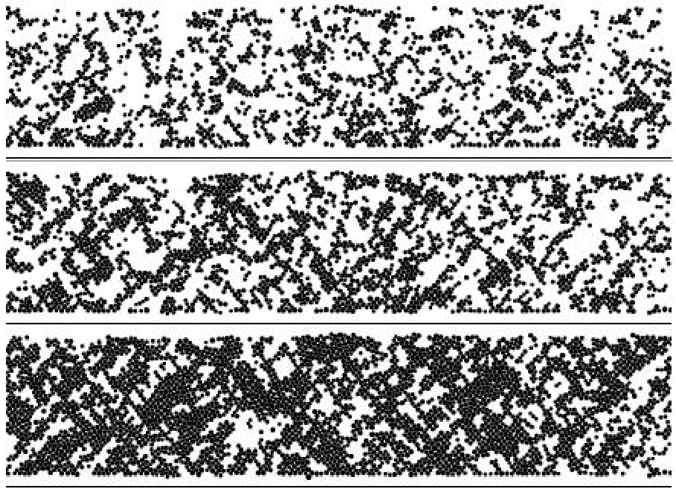

Figure 4. Snapshots of the pile for $\theta = 0°$, $10°$ and θ_c. In black are represented the overloaded grains satisfying $\gamma \geqslant \Gamma_c$, where $\gamma = q/p$ is computed from the grain moment tensor.

points $\boldsymbol{r}^\alpha$ (Figure 2). The moment tensor $\boldsymbol{M}_p$ of the grain p is given by:

$$M_{ij}(p) = \sum_{\alpha=1,N_\alpha} r_i^\alpha f_i^\alpha, \qquad (1)$$

where i and j are the space dimensions. Using the additivity of the moment tensor, we compute the tensor $\boldsymbol{M}$ of the pile taking into account all the grains. The moment tensor is related to the stress tensor through the relation $\boldsymbol{\sigma} = \boldsymbol{M}/V$ where V is the volume over which the tensor is evaluated. In the following we consider ratios of stress component so that the definition of the volume is not required. Using the eigen values of the moment tensor m_1 and m_2, we compute the deviatoric part $Q = (m_1 - m_2)/2$ and the isotropic part $P = (m_1 + m_2)/2$. We form the ratio of these two quantities

$$\Gamma = \frac{Q}{P}, \qquad (2)$$

i.e. the level of deviatoric stress normalised by the pressure.

3.2 *Macroscopic stress and grains stresses*

The evolution of the ratio Γ evaluated over the whole volume of the pile as a function of the slope angle θ is reported in Figure 3. While the slope evolves towards θ_c, the linear increase of Γ shows the gradual loading of the slope and the increase of shear stress. For $\theta \simeq 19.5°$, this regular increase stops and softening of the material occurs; this indicates that the stability limit is reached, namely that $\theta = \theta_c$. We define the corresponding limit stress state

$$\Gamma_c = \frac{Q}{P}(\theta_c). \qquad (3)$$

The mechanism by which the whole pile reaches the limit state Γ_c is not obvious. In order to compare this

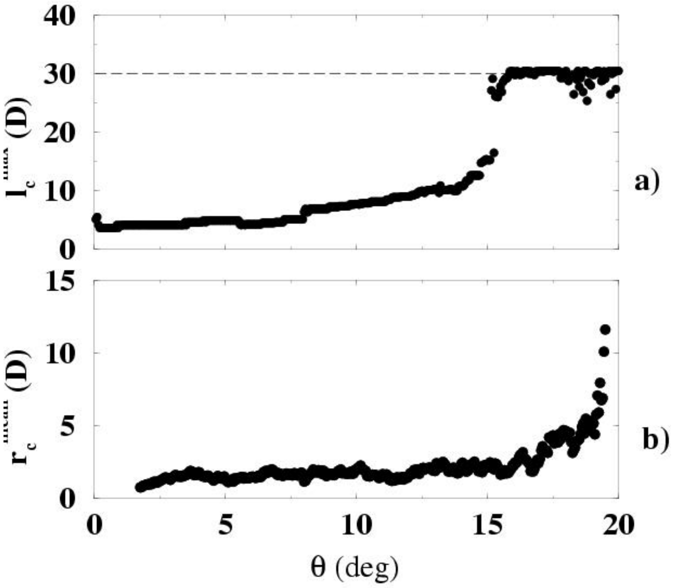

Figure 5. Evolution of the maximum size of the areas where the stress state satisfies $\Gamma = \Gamma_c$ (graph a) and evolution of the mean size of the areas where the mobilisation of friction satisfies $\nu = \nu_c$ (graph b) as a function of the slope θ.

macroscopic evolution to the evolution of the stress state at the grains scale, we define for each grain the stress ratio

$$\gamma = \frac{q}{p}, \tag{4}$$

where q and p are the deviatoric and isotropic part of the grain moment tensor given by equation (1). We focus on the *overloaded grains*, namely the grains satisfying $\gamma \geqslant \Gamma_c$. Three snapshots of the pile for $\theta = 0$, $10°$ and θ_c are shown in Figure 4; on these snapshots, the overloaded grains only are represented in black. In the course of time, we observe a slow structuring of the packing very much reminiscent of a percolation process.

3.3 *Multi-scale analysis*

The structuring of the local stress state corresponds to the slow emergence of areas where the stress state has locally reached the macroscopic limit Γ_c. We compute the maximum size ℓ_c^{max} of these areas in the course of time. To do so, we focus on the overloaded grains; for each one, we consider a circular neighborhood of radius ℓ over which the stress state is evaluated. We can thus determine the size of the neighborhood ℓ_c for which the stress state satisfies $\Gamma = \Gamma_c$. Carrying this operation over all the overloaded grains we are able to determine $\ell_c^{max} = \max\{\ell_c\}$ for any value of the slope θ. The evolution of ℓ_c^{max} as a function of θ is plotted in Figure 5a. We first observe a slow increase for $\theta \in [0, 15°]$. At $\theta \simeq 15°$, a rapid jump suddenly brings ℓ_c^{max} to $30D$, namely a size comparable to the packing height (this maximum value $30D$ is imposed as a cut-off for practical reasons in the computation of ℓ_c, which otherwise would reach the pile dimension $40D$). Again, this behaviour is reminiscent of a

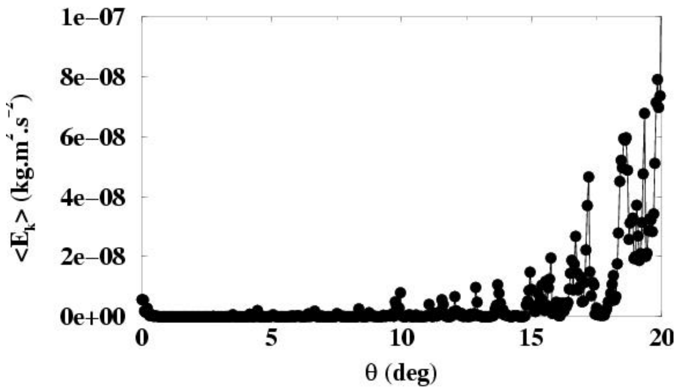

Figure 6. Mean kinetic energy of the grains as a function of the slope angle θ. We observe increasing peaks when $\theta \to \theta_c$.

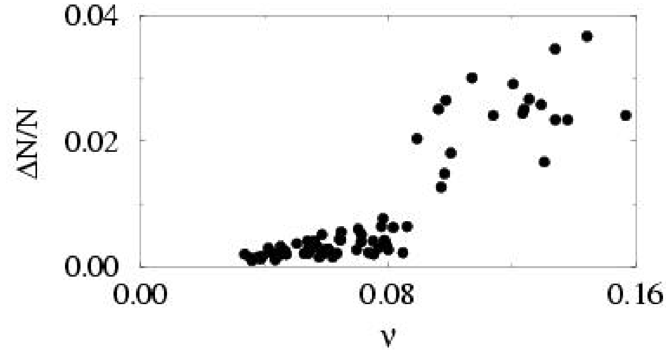

Figure 7. Size of the friction-driven instabilities as a function of the density of critical contacts ν. We observe two different behaviours depending on if $\nu \leqslant \nu_c$ or $\nu \geqslant \nu_c$, with $\nu_c \simeq 0.08$.

percolation mechanism. Moreover, it clearly establish the existence of a transition in the state of the packing few degrees (here $5°$) before the angle of avalanche θ_c is reached. Beyond the fact that this transition in itself is a strong precursor of the avalanche, it changes the internal state of the packing and presumably its susceptibility to avalanching.

4 AVALANCHE PRECURSORS

4.1 *The mobilization of contact friction*

The friction acting between the grains is a simple Coulomb law relating the normal and tangential force at contact N and T through the relation $T/N \leqslant \mu$, where μ is the microscopic coefficient of friction. When the Coulomb threshold is reached, namely for $T/N = \mu$, any relative slip motion between the two grains in contact is possible. Such slip motions create a local dynamical instability which allows for the local reorganization of the packing: collective slip motions and redistribution of the forces. These instabilities release energy and help the pile finding a more stable configuration; however, the perturbation they create may not be damped by the rearrangements of the grains and a surface avalanche might be triggered. The kinetic energy released by these friction-induced instabilities is reported in Figure 6 as a function of the slope angle θ. We observe peaks increasing in size at the approach of the stability limit. It can be

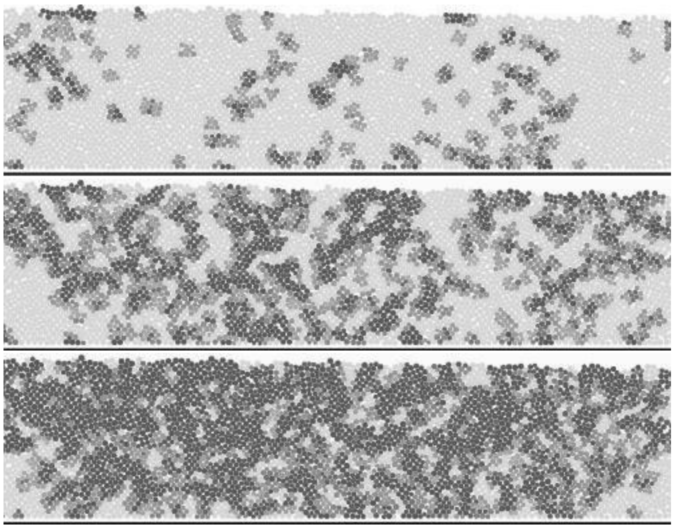

Figure 8. Snapshots of the pile for $\theta = 10°$, $16°$ and θ_c. In black are represented the areas where the critical contact density satisfies $\nu \geqslant \nu_c$.

shown that the occurrence of the dynamical instabilities is related to the mobilization of the contact friction forces (Staron *et al* 2002). We define the proportion ν of contact satisfying $T/N = \mu$ (referred to as *critical* in the following):

$$\nu = \frac{N_c}{N},$$

where N_c is the number of critical contacts and N is the total number of contacts in the packing. We can show that ν is bounded by a saturation value ν_c for which the probability of larger scale instabilities becomes higher. This behaviour is apparent when plotting the size of the instability as a function of the proportion of critical contacts (*i.e.* in the state $T/N = \mu$) reached just before the instability (Figure 7). The size of the instability is measured as the proportion of contacts gained or lost in the event. Two clouds of points can be distinguished: a group of frequent small-scale rearrangements for $\nu \leqslant \nu_c$, and a group of rare large-scale rearrangements for $\nu \geqslant \nu_c$.
In Figure 8 are presented three snapshots of the state of the pile for $\theta = 10°$, $16°$ and θ_c. The gray scale encode the local density of critical contacts; areas represented in black have reached the state $\nu \geqslant \nu_c$, and are thus potential source of friction-induced instabilities. We observe that these areas grow in size and finally span the whole pile when stability limit approaches, following a process again bearing strong analogy with percolation. The evolution of the mean size r_c^{mean} of these areas where $\nu \geqslant \nu_c$ is plotted in Figure 5b as a function of the slope angle θ. A divergence is clearly observed in the interval of slope angle $[16°, \theta_c]$. As previously, we observe that the internal state of the pile (here the organization of contact friction) undergoes a dramatic evolution few degrees before the angle of avalanche is reached.

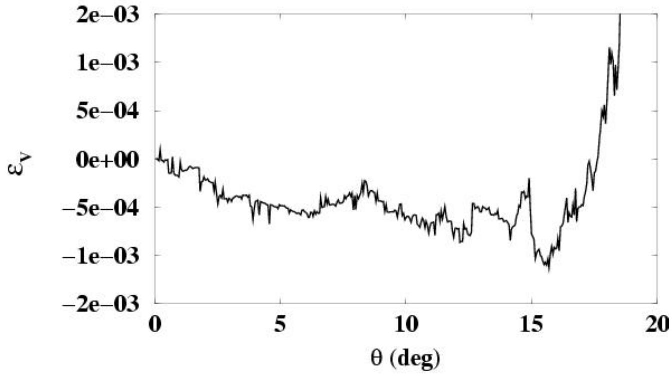

Figure 9. Variations of the packing volume $\epsilon_V = (V - V_0)/V_0$ as a function of the slope angle θ. We observe a period of contractant behaviour followed by dilatancy after $\theta \approx 15°$.

4.2 *The dilatancy transition*

We measure the variations of the volume of the packing $\epsilon_V = (V - V_0)/V_0$, where V_0 is the initial volume, as a function of the slope angle θ. These variations are plotted in Figure 9. We first observe a contractant behaviour followed by a dilatant behaviour as is classically observed in dense sands. Remarkably, the transition to dilatant behaviour occurs at $\theta \simeq 15°$, in coincidence with the transition in the stress state and the contact friction mobilization.

5 CONCLUSIONS

Using numerical simulation, we have shown the existence of a sharp transition in the state of a granular slope few degrees before the angle of avalanche. This transition involve the packing micro-structure, namely the local stress and the contact friction. It is accompanied by avalanche precursors *i.e.* local dynamical instabilities and a dilatant behaviour. This transition involved a mechanism very reminescent of percolation process, thus stressing the analogy between granular slopes loss of stability and phase transition. Interestingly, this transition coincides with a transition towards a metastable state observed experimentally. It is not clearly established whether this sharp modification of the local stress and of the microscopic friction results in the emergence of new correlation lengths in the packing. Nevertheless, it is very tempting to identify the origin of the metastability with these modifications of the internal state of the pile.

REFERENCES

Daerr, A. & Douady, S. 1999, Two types of avalanche behaviour in granular media, *Nature* **399**, pp. 241-243

Deboeuf, S., Bertin, E. M., Lajeunesse, E. & Dauchot, O. 2003, Jamming transition of a granular pile below the angle of repose, *Eur. Phys. J B* **36**, pp. 105-113

Jean, M. & Moreau, J.-J. 1992, Unilaterality and dry friction in the dynamics of rigid body collections, *Proceedings of Contact Mechanics International Symposium*, pp. 31-48

Moreau, J.-J. 1997, Numerical investigation of shear zones in granular materials, *Friction, Arching, Contact Dynamics*, World Scientific Publishers, pp. 233-247

Staron, L., Vilotte, J.-P. & Radjai, F. 2002, Pre-avalanche instabilities in a granular pile, *Phys. Rev. Lett.*, **89**, p. 204302-1

Staron, L., Vilotte, J.-P. & Radjai, F. , Multiscale analysis ot the stress state in a granular slope in transition to failure, *Phys. Rev. E submitted, condmat/0409619*